RSC Advances

PAPER

View Article Online
View Journal | View Issue

Cite this: *RSC Adv.*, 2017, **7**, 4547

Room-temperature pulsed CVD-grown SiO_2 protective layer on TiO_2 particles for photocatalytic activity suppression

Jing Guo,[ab] Shaojun Yuan,[a] Yangyang Yu,[a] J. Ruud van Ommen,[b] Hao Van Bui[b] and Bin Liang*[a]

Received 9th December 2016
Accepted 3rd January 2017

DOI: 10.1039/c6ra27976g

www.rsc.org/advances

This work presents a novel chemical vapor deposition (CVD) approach that enables the deposition of ultrathin and conformal SiO_2 layers on TiO_2 anatase nanoparticles at room temperature using $SiCl_4$ and air containing water without the use of a catalyst. The morphology of the CVD-grown SiO_2 layers was found to be strongly dependent on the initial surface states of the TiO_2 nanopowders, which could be altered by applying a simple heat pretreatment. The deposition on untreated TiO_2 resulted in granular films, whereas on preheated TiO_2 highly uniform and conformal SiO_2 layers were obtained. By varying the $SiCl_4$ precursor dosing time and the number of CVD cycles, the thickness of the SiO_2 could be controlled at the nanometer level, which allowed us to investigate the influence of film thickness on the photocatalytic suppression ability. We found that a conformal SiO_2 layer with a thickness of 3 nm could sufficiently suppress the photocatalytic activity of anatase TiO_2 nanoparticles, which was demonstrated by the photodegradation of Rhodamine B. Our approach offers a simple, fast, feasible and low-temperature deposition method which can be directly applied to SiO_2 coating on nanoparticles in pigments and other fields, particularly heat-sensitive materials, and further developed for large-scale production.

1 Introduction

Nanoparticulate titanium dioxide (TiO_2) is the most commonly-used white pigment in the paint, plastic, and paper industries due to its high brightness, high refractive index and photostability.[1,2] However, the high photocatalytic activity of TiO_2 facilitates the oxidation and decomposition of organic compounds, for instance, in the paint layer, which consequently changes the color and severely decreases the lifetime of the products.[3] Therefore, in these practical applications, TiO_2 nanoparticles (NPs) are commonly coated with a thin insulating layer to suppress their photocatalytic activity. On the one hand, this coating layer is required to sufficiently block the transport of electrons and holes, which are generated in the TiO_2 particles under UV-light irradiation, to the surface that initiates the photocatalytic reactions with organic compounds. On the other hand, the coating layer must not affect the bulk optical properties of the TiO_2 pigment. Owing to their large band gap, high thermal and optical stabilities, and chemical inertness, ceramic oxides, such as Al_2O_3, SiO_2, CeO_2 and ZrO_2, have been popularly used as coating materials on TiO_2 for photocatalytic suppression.[4–14]

Various strategies have been developed to deposit thin metal oxide films on TiO_2 pigment particles. Among them, wet chemistry methods, such as sol–gel and precipitation, have been extensively used due to their simplicity, inexpensiveness and versatility in producing various materials with tunable properties.[4–6,8,15,16] For instance, Ren *et al.* employed sol–gel method in the presence of 3-hydroxytyramine hydrochloride, poly(-diallyldimethylammonium chloride), poly(sodium 4-styreneslfonate), tetraethyl orthosilicate (TEOS) and solvents to fabricate TiO_2/SiO_2 core/shell particles.[6] Upon exposure to UV radiation, a rattle-type structure with tunable catalytic/UV-shielding properties was obtained. The TiO_2/SiO_2 core/shell structure for UV radiation shielding can also be obtained by the conventional Stöber method using TEOS and solvents such as ethanol, NH_4OH and acetone.[4,5] Binary Al_2O_3/SiO_2 coating layers have been deposited on TiO_2 nanoparticles using sol–gel and precipitation mothods for enhanced brightness and whiteness of TiO_2.[8,16] Moreover, wet chemistry methods enable the deposition of various ceramic and transition metal oxide materials such as ZrO_2, CeO_2, NiO and CoO on TiO_2 particles.[15] Nevertheless, these methods have several shortcomings in controlling the coating thickness and conformality due to their high sensitivity to experimental parameters, such as precursor concentration, type and pH of the solvents, deposition time and temperature. In

[a]*Multi-phase Mass Transfer & Reaction Engineering Lab, College of Chemical Engineering, Sichuan University, Chengdu 610065, China. E-mail: liangbin@scu.edu.cn; Fax: +86-28-85460556; Tel: +86-28-85460556*

[b]*Department of Chemical Engineering, Delft University of Technology, Delft, The Netherlands*

addition, these methods are time consuming and normally require post-treatment processes, for instance, high temperature treatment, washing, drying, and separation to eliminate impurities that arise from the residual solvent and reaction byproducts.[5,6] These disadvantages hinder the applicability of wet chemistry in the syntheses of metal oxide layers on TiO_2 in practical applications. It is therefore of importance to search for a facile, low-cost, and efficient approach for deposition of metal oxide layers on the TiO_2 particles.

Gas-phase deposition techniques such as chemical vapor deposition (CVD) and atomic layer deposition (ALD) have been attractive alternatives in recent years. ALD is based on the sequential exposures of the support/substrate to precursors in the gas phase. This enables self-limiting surface reactions and provides the ability to control the amount of depositing materials down to atomic level with high uniformity and conformality in many applications.[17,18] ALD has also been applied for coating Al_2O_3 and SiO_2 films on TiO_2 nanoparticles for catalytic suppression.[12–14] With ALD, ultrathin and conformal SiO_2 and Al_2O_3 layers with a thickness of several nanometers can be achieved, showing excellent stability and high efficiency in suppressing the catalytic properties of TiO_2 nanoparticles.[12,13] Molecular layer deposition (MLD), the organic counterpart of ALD, has also been applied for depositing aluminum alkoxide (*i.e.*, alucone) using trimethylaluminum and ethylene glycol as precursors. This alucone layer can reduce the undesired color change of the white pigment TiO_2, which was observed for the TiO_2 coated with SiO_2 and Al_2O_3 layers by ALD.[14]

CVD of SiO_2 thin films has been extensively investigated over the past decades.[10,11,19–25] TEOS, silane (SiH_4), dichlorosilane ($SiCl_2H_2$) and silicon tetrachloride ($SiCl_4$) are among the most popularly used precursors in conjunction with H_2O or O_2 as oxidizing agent. This has been used to deposit thin SiO_2 layers on TiO_2 micro- and nanoparticles.[10,23,26,27] Powell *et al.* demonstrated CVD of SiO_2 films at a temperature in the range of 1300–1500 °C employing the $SiCl_4/O_2$ chemistry, and found that the film surface was smoother at a higher temperature and in the absence of water.[11,26,27] Using the same $SiCl_4/O_2$ chemistry, Simpson *et al.* reported that ultrathin and continuous SiO_2 layers with a thickness of 1–2 nm could be obtained at 1000 °C.[10] By replacing O_2 with H_2O as the oxidizing agent, Tsapatsis and Gavalas demonstrated that the deposition temperature of SiO_2 CVD could be significantly reduced to approximately 600 °C.[23] It can be concluded that CVD of SiO_2 generally requires an elevated temperature. Remarkably, Klaus and George found that the use of NH_3 as catalyst for the $SiCl_4/H_2O$ CVD process could enable the deposition of SiO_2 at room temperature.[24] To the best of our knowledge, this is so far the only room-temperature SiO_2 CVD process using $SiCl_4$ precursor reported in literature.

Accordingly, the main aim of this work is to develop a novel approach that enables the room-temperature CVD (RTCVD) of SiO_2. We demonstrate that ultrathin and conformal SiO_2 layers on TiO_2 nanoparticles can be deposited at room temperature using $SiCl_4$ and air containing water without the use of catalysts. As $SiCl_4$ can react robustly with H_2O, the use of air containing water is to decelerate the reaction kinetics and achieve a better control of deposition rate. Therefore, the thickness of coating layers can be controlled at nanometer scale by varying the $SiCl_4$ dosing time and the number of CVD cycles. We found that the morphology of the coating layers, *i.e.*, granular or continuous films, is strongly influenced by initial surface states of the TiO_2 nanopowders, which can be altered by applying a simple heat treatment at a relatively low temperature (*i.e.*, 170 °C). Photocatalytic tests are performed on the as-synthesized SiO_2/TiO_2 nanoparticles to evaluate the catalytic suppression ability of the room-temperature CVD-grown SiO_2, and to study the influence of coating thickness on the suppression ability. The results obtained from our work demonstrate a simple, fast and feasible method for coating SiO_2 on TiO_2 pigment, which is applicable for other powders and can be further developed for large-scale production.

2 Experimental

2.1. Materials

Anatase TiO_2 powders with diameter in the range of 200–300 nm and specific surface area of about 10.7 $m^2\ g^{-1}$ (determined by BET technique) were provided by Taihai TiO_2 pigment Co. (Panzhihua, China). Rhodamine B (RhB) and silicon tetrachloride ($SiCl_4$) were purchased from Sigma-Aldrich (St. Louis, MO, USA). The TiO_2 powders and the chemicals were used as received without any additional treatment or purification.

2.2. Preparation of SiO_2-coated TiO_2 nanoparticles

The coating apparatus and deposition steps are schematically shown in Fig. 1. TiO_2 powders, without or with heat pretreatment at 170 °C for 1 h (*i.e.*, performed *ex situ* in an oven prior to the CVD), were supported on a porous distributor plate, and were immobilized inside a glass reactor with volume of 1 L (Fig. 1a). The thickness of the TiO_2 layer on the distributor plate is about 2 mm. At this thickness and with a long dosing time (*i.e.*, up to 60 min), the diffusion limitation of the gas molecules to the bottom of the layer can be eliminated.[28] Before introducing $SiCl_4$, the reactor was slowly evacuated to a pressure of 70 mbar using a mechanical pump. This was to create a pressure difference between the chamber and the $SiCl_4$ vapor precursor (*ca.* 260 mbar at room temperature). $SiCl_4$ was then fed into the reactor (V1 opened, V2 and V3 closed) with dosing times varying from 3 to 60 min to react with the hydroxyl groups (–OH) on the surface of TiO_2 nanoparticles (Fig. 1b–d). Hereafter, the excess precursor, if any, and the reaction byproducts (*i.e.*, HCl) were removed (V1 and V2 closed, V3 opened). Air containing H_2O vapor (*i.e.*, 44% RH) was then introduced into the chamber and maintained at atmospheric pressure to react with the Si–Cl terminated surface, forming an SiO_2 layer and creating an –OH terminated surface (Fig. 1e), which is necessary for the chemisorption of $SiCl_4$ in the next cycle. The use of air containing H_2O vapor instead of pure H_2O is due to the fact that $SiCl_4$ can react robustly with H_2O, which could lead to the uncontrollable deposition.

2.3. Material characterization

The thickness of the SiO_2 layers on the TiO_2 particles was measured by transmission electron microscopy (TEM) using

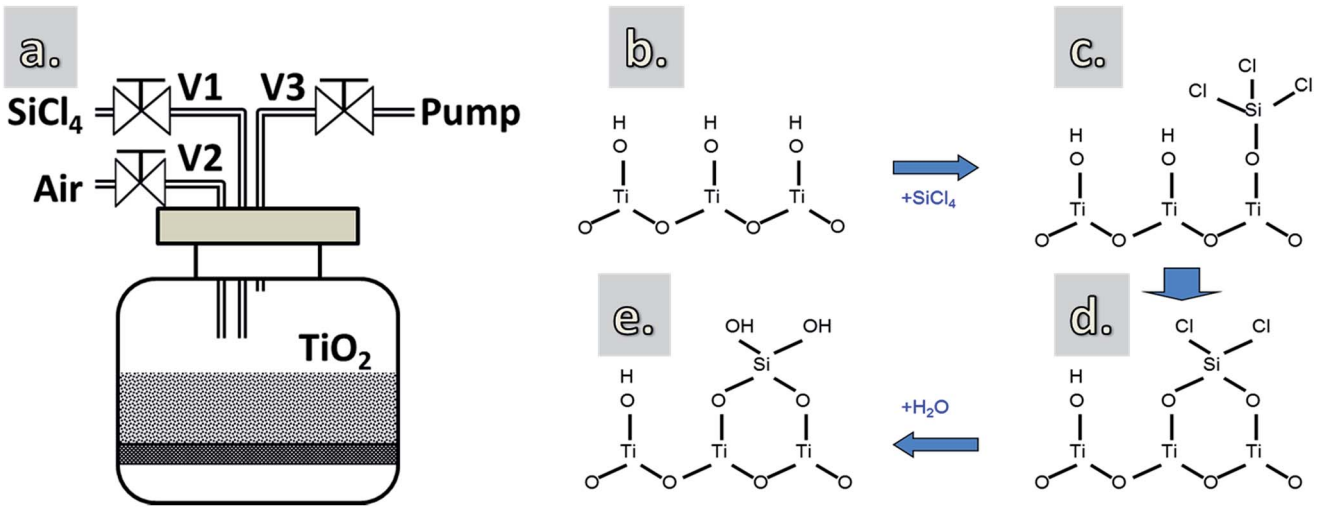

Fig. 1 A schematic drawing of the reactor (a) and the proposed growth mechanism of SiO_2 using $SiCl_4$ and H_2O vapor (b–e).

a JEOL JEM1400 operating at a voltage of 120 kV and a current density of 50 pA cm^{-2}. The composition of the SiO_2 layers was characterized by X-ray photoelectron spectroscopy (XPS) (XSAM800, Kratos, UK) with monochromatized Al Kα radiation at constant dwell time of 100 ms and pass energy of 55 eV. The peaks positions were calibrated according to the C 1s peak at 284.8 eV. The infrared spectra were acquired using FTIR spectroscopy (Spectrum II L1600300 spectrometer, PerkinElmer) in transmission mode.

2.4. Photocatalytic activity determination

The photocatalytic activity of the SiO_2-coated TiO_2 powders was evaluated by the photodegradation of RhB solution. For each test, 150 mg powders were added to 30 mL RhB solution (concentration of 9 mg L^{-1}) and continuously stirred in the dark for 30 min to obtain a uniform suspension. Thereafter, the suspension was exposed to UV radiation generated by a mercury lamp with a power of 300 W or 500 W for different exposure times. The set-up allowed to carry out up to 10 samples simultaneously, which ensured that all samples were irradiated under the same conditions, such as light intensity, exposure time, and temperature. The suspension was then centrifuged to separate the powders from the solution. Finally, the solution was analyzed by UV-visible spectrophotometry to determine the residual concentration of the RhB in solution, which was used to evaluate the catalytic activity suppression of the SiO_2 layers.

3 Results and discussion

3.1. Reaction mechanism

The chemical reactions in CVD of SiO_2 using $SiCl_4$ and H_2O are generally described as:[24]

$$SiCl_4 + 2H_2O \rightarrow SiO_2 + 4HCl \quad (1)$$

However, it has been reported that the actual growth of SiO_2 CVD consists of a number of reactions, which can be divided into homogeneous and heterogeneous reactions.[22,23] Homogeneous reactions occur between $SiCl_4$ and H_2O molecules in the gas phase, forming oligomers or particles. These reactions have slow kinetics.[22,23,29] The heterogeneous reactions take place directly on the surface *via* substitution reactions of surface groups (*i.e.*, –Cl and –OH groups). In this case, the reactions are described as:[22,23]

$$|\text{–OH(s)} + SiCl_4(g) \rightarrow |\text{–O–Si–Cl(s)} + HCl(g) \quad (2)$$

$$|\text{–O–Si–Cl(s)} + H_2O(g) \rightarrow |\text{–O–Si–OH(s)} + HCl(g) \quad (3)$$

where |–OH(s) and |–Si–Cl(s) represent the surface hydroxyl and chlorosilicon groups, respectively. In addition to these reactions, condensation reactions simultaneously take place between two –OH groups or –OH and Si–Cl groups on the surface to form siloxane bonds (Si–O–Si), described as:[22,23]

$$|\text{–O–Si–OH(s)} + |\text{–O–Si–Si–OH(s)} \rightarrow \text{Si–O–Si(s)} + H_2O(g) \quad (4)$$

$$|\text{–O–Si–OH(s)} + |\text{–O–Si–Si–Cl(s)} \rightarrow \text{Si–O–Si(s)} + HCl(g) \quad (5)$$

Therefore, CVD of SiO_2 using $SiCl_4$ and H_2O might consist of gas-phase reactions, substitution reactions of surface functional groups and condensation reactions.

3.2. Morphology and composition of the coating layers

Tsapatsis *et al.* postulated that the surface morphology of the coating layer is influenced by the reactant species, *i.e.*, H_2O molecules (vapor and physisorbed H_2O) and –OH groups (chemisorbed H_2O). Accordingly, the reactions between $SiCl_4$ and H_2O molecules may lead to the formation of a granular surface.[22,23] However, this has not been experimentally demonstrated. Here, we observed that the deposition of SiO_2 on TiO_2 particles without pretreatment resulted in granular and porous surfaces (Fig. 2a). This is attributed to the presence of a thick hydration shell with abundant physisorbed H_2O and –OH groups on the particle surface,[30] as detected by FTIR spectra (Fig. 2c). The peak at 3400 cm^{-1} is attributed to the stretching vibration of –OH groups (ν_{O-H}) on the surface of TiO_2 particles, whereas the peak at

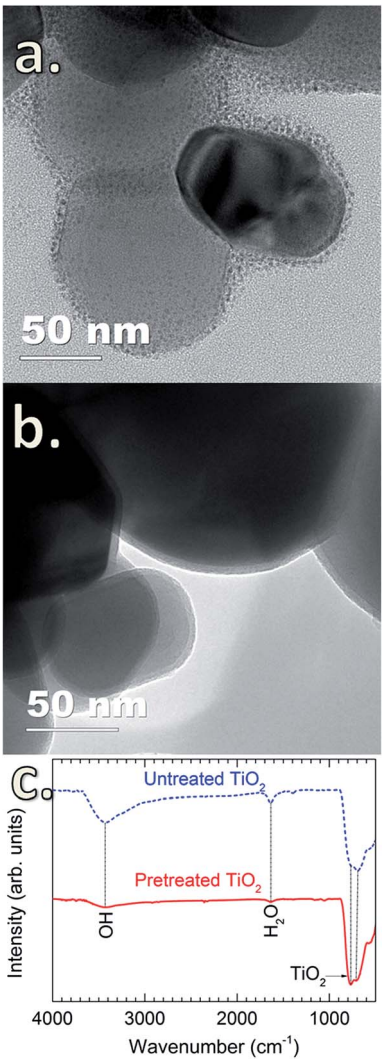

Fig. 2 TEM images of SiO_2-coated anatase TiO_2 particles (a) without heat pretreatment and (b) with heat pretreatment at 170 °C for 1 h, and (c) FTIR spectra of the SiO_2-coated TiO_2 particles without and with heat pretreatment. CVD reaction conditions: $SiCl_4$ dosing time of 60 min and air exposure time of 60 min. The average thickness of the SiO_2 coating layer is 3.4 ± 0.1 nm.

1625 cm^{-1} corresponds to the bending vibration of physisorbed H_2O molecules (δ_{H_2O}).[31,32] In the fingerprint region (*i.e.*, wavenumber below 1000 cm^{-1}), the peaks located in the wavenumber range of 500–700 cm^{-1} are ascribed to the bending vibration of Ti–O–Ti ($\delta_{Ti-O-Ti}$) of the TiO_2 particles.[31] Upon the heat pretreatment of TiO_2 particles at 170 °C for 1 h, the intensity of the characteristic peaks of ν_{O-H} and δ_{H_2O} significantly decreases (Fig. 2c), indicating that a large amount of the physisorbed H_2O molecules and –OH groups has desorbed from the TiO_2 surface.[33–37] Therefore, for the untreated TiO_2 particles, the physisorbed H_2O can react with $SiCl_4$ to form SiO_2 following reaction (1), and in accordance with the previous assumption by Tsapatsis *et al.*, a granular film is formed.[22] In comparison with the previous findings that the reaction between $SiCl_4$ and H_2O either required high temperatures[22] or the presence of catalysts to enable the deposition at room temperature,[24] our work has demonstrated the deposition of SiO_2 at room temperature without the use of catalyst. This is probably due to the higher pressure range in the reactor, as well as the catalytic TiO_2 surface. Klaus and George also observed that increasing H_2O partial pressure resulted in the enhanced deposition of SiO_2 in $SiCl_4$/H_2O CVD.[24] Nevertheless, this requires further studies to verify, which is out of the scope of this work. On the pretreated TiO_2 particles, highly uniform, continuous and dense SiO_2 films are formed (Fig. 2b), which is substantially different from the porous and granular SiO_2 films on the untreated TiO_2 particles. This is ascribed to the different reaction mechanism. CVD of SiO_2 on the pretreated TiO_2 particles proceeds following the reactions (2)–(5) (*i.e.*, *via* surface reactions with |–OH and |–Cl groups), thus resulting in the formation of continuous and dense layers.

Fig. 3 shows the O 1s and Ti 2p core-level XPS spectra of uncoated and SiO_2-coated TiO_2 powders. For the uncoated TiO_2, the O 1s spectrum is fitted to two peaks with binding energies (BE) at 529.5 and 530.8 eV (Fig. 3a) corresponding to the O–Ti and O–H chemical states, respectively.[38] This is consistent with the results obtained from FTIR shown in Fig. 2c. The O 1s spectrum of the SiO_2-coated TiO_2 shows a noticeable difference with an intense peak at 532.69 eV, representing the Si–O chemical state in SiO_2.[39] The fitted spectrum also reveals the presence of additional components located at 534.5 eV (Si–O_x) and 531.64 eV (Si–O–Ti).[39] No significant change was observed for the Ti 2p spectra of uncoated and SiO_2-coated TiO_2 particles. In addition, no considerable amount of Cl contamination was detected by XPS, suggesting the complete consumption of –Cl by the chemical reactions with H_2O.

The presence of SiO_2 is additionally confirmed by the FTIR spectra obtained for TiO_2 powders coated with SiO_2 layers with different $SiCl_4$ dosing times (Fig. 4). The characteristics of SiO_2 are represented by the two sharp peaks at 1227 and 1080 cm^{-1}.[5] The results show that the absorption increases drastically with the increase of $SiCl_4$ dosing time from 3 to 30 min, which is indicative of the increase of the coating thickness consistent with the results obtained from TEM (Fig. 5). The images indicate that highly uniform and conformal SiO_2 layers with a thickness as thin as 1 nm can be achieved, which is commonly difficult to obtain by conventional CVD. With increasing dosing time from 7 to 30 min, the coating thickness rises rapidly from 1.4 to 3.0 nm, and gradually reaches saturation with the further increase of dosing time. This saturation may be caused by the complete consumption of the –OH functional groups and adsorbed H_2O on the surface by $SiCl_4$, which consequently terminates the chemical reactions. A small increase in thickness with increasing dosing time from 30 to 60 min is attributed to the contribution of the residual H_2O vapor inside the chamber and the condensation reactions described above (*i.e.*, reactions (4) and (5)).

3.3. Catalytic suppression of SiO_2 coating layers

Fig. 6a shows the photocatalytic activity toward the degradation of RhB of the uncoated TiO_2 and the TiO_2 coated with SiO_2 layers obtained for different $SiCl_4$ dosing times. Prior to the UV irradiation, the solution was constantly stirred in the dark (light-off stage) for 30 min to obtain uniform particle dispersion. The

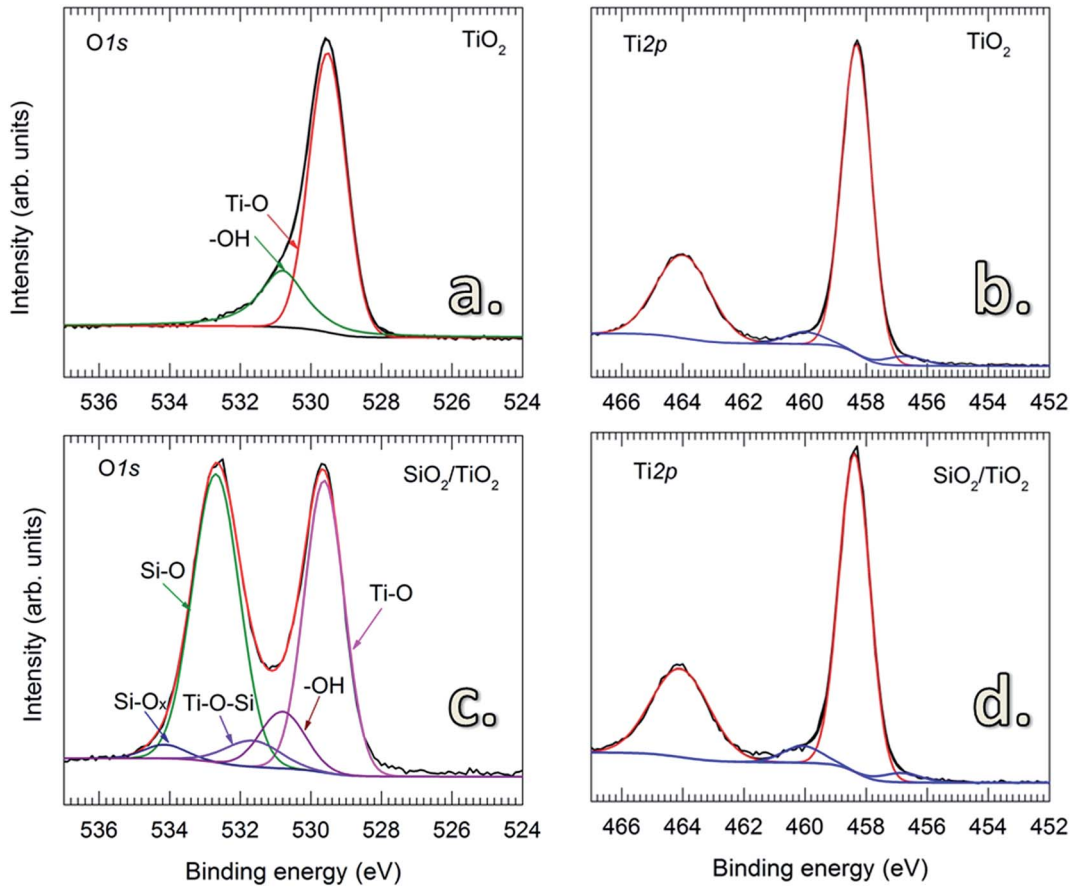

Fig. 3 XPS spectra of O 1s and Ti 2p of uncoated (a and b) and SiO_2-coated TiO_2 (c and d) powders. CVD was performed on pretreated TiO_2 particles with $SiCl_4$ dosing time of 15 min and air exposure time of 60 min.

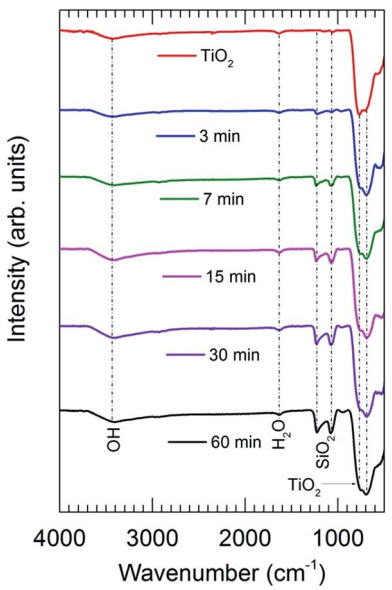

Fig. 4 FTIR spectra of the uncoated TiO_2 and SiO_2-coated TiO_2 with different $SiCl_4$ dosing times. CVD was performed on pretreated TiO_2 particles with an air exposure time of 60 min.

samples were collected after certain time-intervals to determine the concentration of the remaining RhB. In the absence of TiO_2 powders, the results show that during this stage, the concentration of RhB remained unchanged. However, a small drop of RhB concentration was observed for the solutions with TiO_2 powders (both uncoated and coated with SiO_2). This drop is caused by the adsorption of a fraction of RhB molecules on the surface of the particles. Thereafter, upon the exposure to UV radiation (light-on stage), the concentration of RhB decayed rapidly for the uncoated powders, indicating the high photocatalytic activity of TiO_2. Similar effects were observed for the TiO_2 coated with SiO_2 deposited with short $SiCl_4$ dosing times (up to 15 min). This could be due to the insufficient thickness of the coating and/or the devoid pin-hole free films. As shown in Fig. 5a and b, the thickness of the SiO_2 layers for short dosing times is 2 nm or less (*i.e.*, 1.4 and 2.0 nm for 7 and 15 min of dosing time, respectively). SiO_2 films with a thickness of 3 nm and thicker obtained for longer $SiCl_4$ dosing times showed significant improvement in the suppression of TiO_2 photocatalytic activity. The small decrease in RhB concentration observed for these two powders (*i.e.*, with SiO_2 layers obtained for 30 and 60 min $SiCl_4$ exposures) is nearly identical to the decrease observed for RhB without powders, which is attributed to the self-degradation of RhB under the UV irradiation. This is better indicated by the reaction kinetic

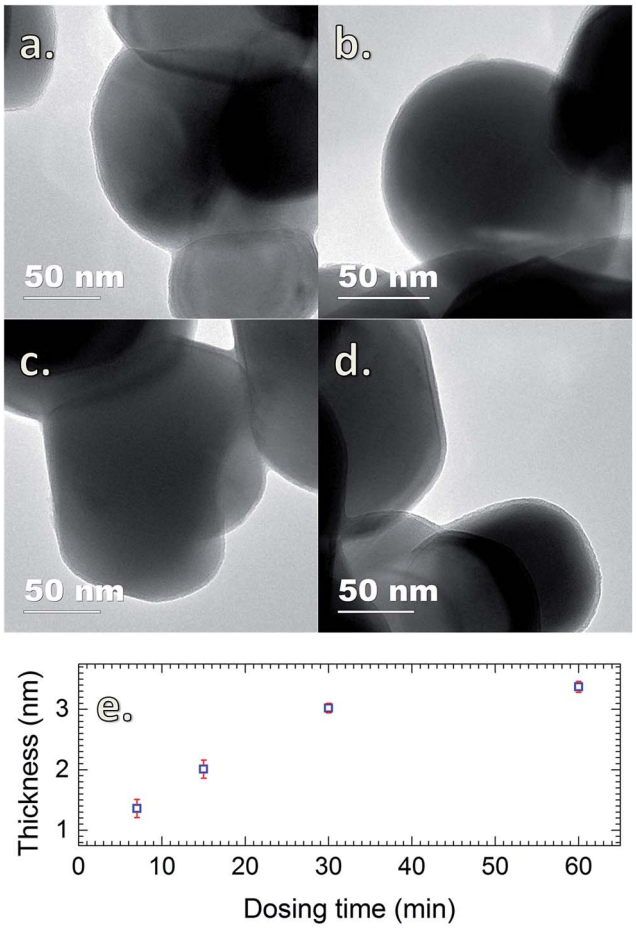

Fig. 5 TEM images of SiO_2-coated TiO_2 particles with different $SiCl_4$ dosing times: 7 min (a), 15 min (b), 30 min (c) and 60 min (d). (e) shows the increasing trend of the coating thickness with dosing time. CVD was performed on pretreated TiO_2 particles.

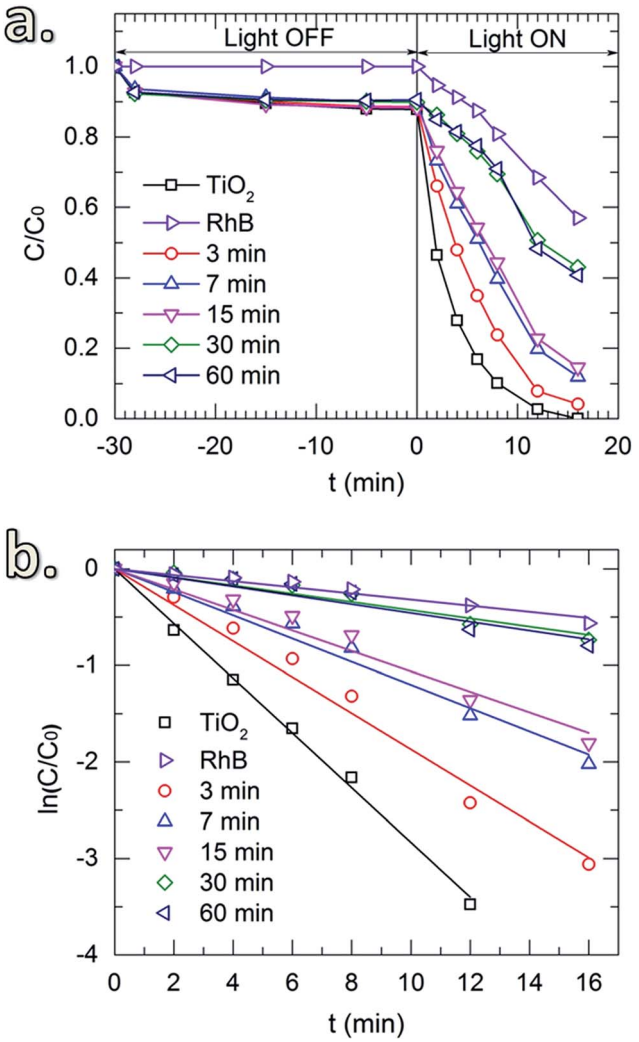

Fig. 6 The photocatalytic degradation of RhB under 500 W UV light using SiO_2-coated TiO_2 powders with different $SiCl_4$ dosing times (a) and the corresponding reaction kinetic plots (b). The k_{app} values are extracted from the slopes of the linear fitting of the measured data.

plots shown in Fig. 6b obtained from the kinetic equation described as:[40]

$$\ln(C_0/C) = k_{app}t, \text{ or } C = C_0 \exp(-k_{app}t) \quad (6)$$

where k_{app} is the apparent first-order kinetic constant, which represents the reaction rate. From eqn (6), k_{app} value for each reaction can be extracted from the slope of the linear fitting (Table 1). The results show that the k_{app} values obtained for the powders coated with SiO_2 with long $SiCl_4$ dosing times are only slightly higher than that of the RhB self-degradation (0.043 and 0.046 compared to 0.032 of RhB), suggesting good catalytic activity suppression by these coatings. In other words, a film thickness of above 3 nm ensures sufficient photocatalytic suppression. The enhancement of the catalytic suppression for the longer dosing time may be ascribed partially to the reconstruction of the layers during the exposure. As discussed above, the small increase in SiO_2 thickness with increasing dosing time might be attributed to the condensation reactions of the precursor molecules (*i.e.*, reactions (4) and (5) in Section 3.1), which create siloxane bonds (Si–O–Si), resulting in fewer pinholes and denser films. This consequently increases the suppression ability of the coating layers. The results from TEM imaging show that the surface morphology of the coating layer was unaffected by the photocatalytic reactions (not shown), indicating the stability of the coating layer.

Table 1 Apparent first-order rate constant, k_{app}, of TiO_2 powders coated with SiO_2 with different $SiCl_4$ dosing times

Dosing time/min	k_{app}/min^{-1}	R^2 of fitting
0 (uncoated TiO_2)	0.283 ± 0.004	0.99
3	0.187 ± 0.006	0.99
7	0.120 ± 0.005	0.99
15	0.106 ± 0.005	0.98
30	0.043 ± 0.003	0.97
60	0.046 ± 0.004	0.95
RhB (without powders)	0.032 ± 0.002	0.98

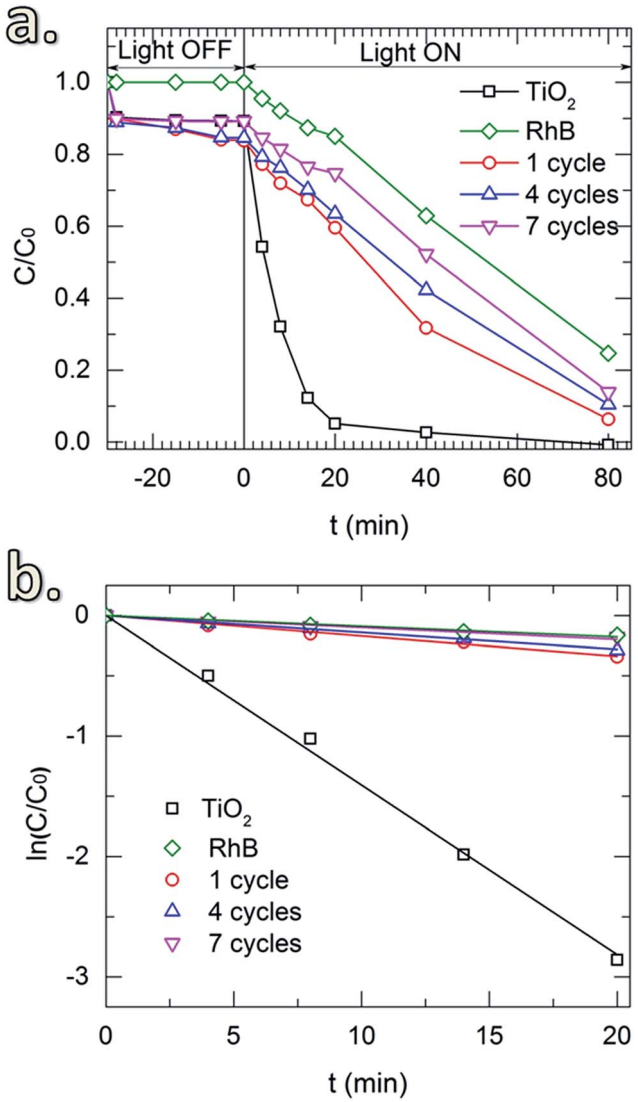

Fig. 7 Photocatalytic degradation of RhB under 300 W UV light using SiO_2-coated TiO_2 powders with different number of SiO_2 CVD cycles (1, 4 and 7). CVD reaction conditions: $SiCl_4$ dosing time of 30 min and air exposure time of 60 min.

Fig. 7 shows the RhB degradation of the SiO_2-coated TiO_2 with different numbers of coating cycles. In this case, an $SiCl_4$ dosing time of 30 min was applied for all of the depositions. Samples for 1, 4 and 7 cycles were tested. In addition, the UV irradiation power was reduced to 300 W to enable the study of the degradation up to 80 min. The same drop of RhB concentration caused by the surface adsorption was observed in the light-off stage (Fig. 7a). In the light-on stage, the reaction kinetic plots (Fig. 7b) show negligible effect of thickness on the photocatalytic degradation, demonstrating the sufficient suppression of the SiO_2 layers deposited with a small number of CVD cycles. In comparison with the materials and coating methods that have been used to mitigate the photocatalytic activity of TiO_2 pigmentary materials (Table 2), our approach showed several advantages in providing a fast, simple and efficient process. Especially, for the first time in literature a room-temperature gas-phase deposition technique for pigmentary coating applications is introduced.

4 Conclusions

We have demonstrated the room-temperature pulsed-CVD of SiO_2 thin films on TiO_2 nanoparticles using $SiCl_4$ as the Si precursor and air containing water vapor as the oxidizing agent without the use of catalysts. The formation of SiO_2 was confirmed by XPS and FTIR spectroscopy. The deposition on the TiO_2 powders without preheating resulted in a granular surface, whereas on pretreated TiO_2 (at 170 °C for 1 h) highly uniform, conformal and continuous SiO_2 films were obtained. The thickness of the SiO_2 layer increased with $SiCl_4$ dosing time and reached saturation most likely upon the consumption of the surface hydroxyl groups and water vapor. This enabled the control of coating thickness at nanometer level precision, and consequently, the study of the influence of film thickness on photocatalytic suppression ability of SiO_2 films. Accordingly, we found that a minimum thickness of about 3 nm is needed to sufficiently suppress the photocatalytic properties of TiO_2

Table 2 Thin film coating methods and materials for suppressing photocatalytic activity of TiO_2 pigmentary materials

TiO_2 material	Coating method	Coating material	Coating thickness (nm)	Deposition temperature (°C)	Photocatalytic reaction	Ref.
P25	ALD	Al_2O_3	6	177	Methylene blue	41
Anatase	ALD	SiO_2	2	500 for SiO_2	IPA to acetone	12
		SiO_2/Al_2O_3	1/1	177 for Al_2O_3		
		$SiO_2/Al_2O_3/SiO_2/Al_2O_3$	0.5/0.5/0.5/0.5			
P25	ALD	Al_2O_3	3.8	150	RhB	42
Anatase	ALD	SiO_2	6	175	Methylene blue	13
P25			9			
Anatase	MLD	Alucone	7–10	100–160	Methylene blue	14
Rutile	CVD	SiO_2	1–2	900–1000	Methylene blue	10
Rutile	Wet-chemistry	ZrO_2	5	40	RhB	15
		CeO_2	1–2	60		
Rutile	Wet-chemistry	CeO_2	1–2	60	RhB	43
ST-21	Wet-chemistry	SiO_2	4	40	Methylene blue	4
P25	Wet-chemistry	Porous SiO_2	20	Room temperature	RhB	6
Anatase	Pulsed-CVD	SiO_2	3	Room temperature	RhB	This work

toward the degradation of RhB. A further increase in film thickness resulted in only insignificant improvement in the suppression performance. Our work has demonstrated a simple, fast and feasible method for depositing SiO_2 on TiO_2 pigment at room temperature, which is applicable also for other powders, especially for heat-sensitive materials, and can be further developed for large-scale production.

Acknowledgements

The authors would like to acknowledge the financial support of key project of National Natural Science Foundation of China (No. 21236004), and China Scholarship Council.

References

1 H. Shi, R. Magaye, V. Castranova and J. Zhao, *Part. Fibre Toxicol.*, 2013, **10**, 15–47.
2 C. L. Bianchi, C. Pirola, F. Galli, G. Cerrato, S. Morandi and V. Capucci, *Chem. Eng. J.*, 2015, **261**, 76–82.
3 X. Feng, S. Zhang and X. Lou, *Colloids Surf., B*, 2013, **107**, 220–226.
4 H. Lee, S. Koo and J. Yoo, *J. Ceram. Process. Res.*, 2012, **13**, S300–S303.
5 O. K. Park and Y. S. Kang, *Colloids Surf., A*, 2005, **257**, 261–265.
6 Y. Ren, M. Chen, Y. Zhang and L. Wu, *Langmuir*, 2010, **26**, 11391–11396.
7 Y. Liu, C. Ge, M. Ren, H. Yin, A. Wang, D. Zhang, C. Liu, J. Chen, H. Feng and H. Yao, *Appl. Surf. Sci.*, 2008, **254**, 2809–2819.
8 Y. Zhang, H. Yin, A. Wang, M. Ren, Z. Gu, Y. Liu, Y. Shen, L. Yu and T. Jiang, *Appl. Surf. Sci.*, 2010, **257**, 1351–1360.
9 H.-X. Wu, T.-J. Wang and Y. Jin, *Ind. Eng. Chem. Res.*, 2006, **45**, 5274–5278.
10 D. J. Simpson, A. Thilagam, G. P. Cavallaro, K. Kaplun and A. R. Gerson, *Phys. Chem. Chem. Phys.*, 2011, **13**, 21132–21138.
11 Q. H. Powell, T. T. Kodas and B. M. Anderson, *Chem. Vap. Deposition*, 1996, **2**, 179–181.
12 D. M. King, X. Liang, B. B. Burton, M. K. Akhtar and A. W. Weimer, *Nanotechnology*, 2008, **19**, 255604–255611.
13 X. Liang, K. S. Barrett, Y.-B. Jiang and A. W. Weimer, *ACS Appl. Mater. Interfaces*, 2010, **2**, 2248–2253.
14 X. Liang and A. W. Weimer, *J. Nanopart. Res.*, 2010, **12**, 135–142.
15 B.-X. Wei, L. Zhao, T.-J. Wang, H. Gao, H.-X. Wu and Y. Jin, *Adv. Powder Technol.*, 2013, **24**, 708–713.
16 B.-X. Wei, L. Zhao, T.-J. Wang and Y. Jin, *Ind. Eng. Chem. Res.*, 2011, **50**, 13799–13804.
17 S. M. George, *Chem. Rev.*, 2010, **110**, 111–131.
18 H. Van Bui, F. Grillo and J. R. van Ommen, *Chem. Commun.*, 2017, **53**, 45–71.
19 F. S. Becker, D. Pawlik, H. Anzinger and A. Spitzer, *J. Vac. Sci. Technol., B*, 1987, **5**, 1555–1563.
20 A. Adams and C. Capio, *J. Electrochem. Soc.*, 1979, **126**, 1042–1046.
21 K. Watanabe, T. Tanigaki and S. Wakayama, *J. Electrochem. Soc.*, 1981, **128**, 2630–2635.
22 M. Tsapatsis, S. Kim, S. W. Nam and G. R. Gavalas, *Ind. Eng. Chem. Res.*, 1991, **30**, 2152–2159.
23 M. Tsapatsis and G. R. Gavalas, *AIChE J.*, 1992, **38**, 847–856.
24 J. W. Klaus and S. M. George, *J. Electrochem. Soc.*, 2000, **147**, 2658–2664.
25 S. Chaudhary, A. R. Head, R. Sánchez-de-Armas, H. Tissot, G. Olivieri, F. Bournel, L. Montelius, L. Ye, F. Rochet, J.-J. Gallet, B. Brena and J. Schnadt, *J. Phys. Chem. C*, 2015, **119**, 19149–19161.
26 Q. H. Powell, G. P. Fotou, T. T. Kodas and B. M. Anderson, *Chem. Mater.*, 1997, **9**, 685–693.
27 Q. H. Powell, G. P. Fotou, T. T. Kodas, B. M. Anderson and Y. Guo, *J. Mater. Res.*, 1997, **12**, 552–559.
28 D. Longrie, D. Deduytsche and C. Detavernier, *J. Vac. Sci. Technol., A*, 2014, **32**, 010802.
29 M. L. Hair and W. Hertl, *J. Phys. Chem. C*, 1969, **73**, 2372–2378.
30 V. N. Koparde and P. T. Cummings, *J. Phys. Chem. C*, 2007, **111**, 6920–6926.
31 S. Musić, M. Gotić, M. Ivanda, S. Popović, A. Turković, R. Trojko, A. Sekulić and K. Furić, *Mater. Sci. Eng., B*, 1997, **47**, 33–40.
32 S. Sivakumar, P. K. Pillai, P. Mukundan and K. G. K. Warrier, *Mater. Lett.*, 2002, **57**, 330–335.
33 S. Benkoula, O. Sublemontier, M. Patanen, C. Nicolas, F. Sirotti, A. Naitabdi, F. Gaie-Levrel, E. Antonsson, D. Aureau, F.-X. Ouf, S.-I. Wada, A. Etcheberry, K. Ueda and C. Miron, *Sci. Rep.*, 2015, **5**, 15088.
34 M. A. Henderson, *Langmuir*, 1996, **12**, 5093–5098.
35 L. Walle, A. Borg, P. Uvdal and A. Sandell, *Phys. Rev. B: Condens. Matter Mater. Phys.*, 2009, **80**, 235436.
36 S. Wendt, R. Schaub, J. Matthiesen, E. K. Vestergaard, E. Wahlström, M. D. Rasmussen, P. Thostrup, L. M. Molina, E. Lægsgaard, I. Stensgaard, B. Hammer and F. Besenbacher, *Surf. Sci.*, 2005, **598**, 226–245.
37 U. Aschauer, Y. He, H. Cheng, S.-C. Li, U. Diebold and A. Selloni, *J. Phys. Chem. C*, 2009, **114**, 1278–1284.
38 B. Erdem, R. A. Hunsicker, G. W. Simmons, E. D. Sudol, V. L. Dimonie and M. S. El-Aasser, *Langmuir*, 2001, **17**, 2664–2669.
39 G. Kovács, Z. Pap, C. Coteț, V. Coşoveanu, L. Baia and V. Danciu, *Materials*, 2015, **8**, 1059–1073.
40 S. Wang, F. Teng and Y. Zhao, *RSC Adv.*, 2015, **5**, 76588–76598.
41 L. F. Hakim, D. M. King, Y. Zhou, C. J. Gump, S. M. George and A. W. Weimer, *Adv. Funct. Mater.*, 2007, **17**, 3175–3181.
42 E. Jang, K. Sridharan, Y. M. Park and T. J. Park, *Chem.–Eur. J.*, 2016, **22**, 12022–12026.
43 H. Gao, B. Qiao, T.-J. Wang, D. Wang and Y. Jin, *Ind. Eng. Chem. Res.*, 2014, **53**, 189–197.

